INL/CON-13-30688
PREPRINT

TEM Characterization of High Burn-Up Microstructure of U-7Mo Alloy

RRFM 2014

J. Gan
B. D. Miller
D. D. Keiser, Jr.
A. Robinson
J. Madden
P. Medvedev
D. Wachs

April 2014

The INL is a
U.S. Department of Energy
National Laboratory
operated by
Battelle Energy Alliance

TEM CHARACTERIZATION OF HIGH BURN-UP MICROSTRUCTURE OF U-7Mo ALLOY

J. GAN, B. D. MILLER, D. KEISER, JR. A. ROBINSON, J. MADDEN, P. MEDVEDEV AND D. WACHS

Nuclear Fuels and Materials Division, Idaho National Laboratory
P. O. Box 1625, Idaho Falls, ID 83415–6188, USA

ABSTRACT

As an essential part of global nuclear non-proliferation effort, the RERTR program is developing low enriched U-Mo fuels (< 20% U-235) for use in research and test reactors that currently employ highly enriched uranium fuels. One type of fuel being developed is a dispersion fuel plate comprised of U-7Mo particles dispersed in Al alloy matrix. Recent TEM characterizations of the ATR irradiated U-7Mo dispersion fuel plates include the samples with a local fission densities of 4.5, 5.2, 5.6 and 6.3 E+21 fissions/cm^3 and irradiation temperatures of 101–136°C. The microstructure of the irradiated U-7Mo fuel particles consists of fission gas bubble superlattice, large gas bubbles, solid fission product precipitates associated with the large gas bubbles, grain subdivision to tens or hundreds of nanometer size, collapse of bubble superlattice, and amorphization. This paper will describe the observed microstructures specifically focusing on the U-7Mo fuel particles. The impact of the observed microstructure on the fuel performance and the comparison of the relevant features with that of the high burn-up UO_2 fuels will be discussed.

1. Introduction

Transmission electron microscopy (TEM) characterization with high-resolution local microstructure and composition analysis in post-irradiation-examination (PIE) provides critical information in understanding the fuel performance in the reactors [1, 2]. With the recent advancement on TEM sample preparation using focused ion beam (FIB) technique for the irradiated fuels, site-specific TEM analysis from the areas of interest identified from scanning electron microscopy (SEM) become routinely available for the irradiated fuels [3]. TEM and SEM are two powerful complementary characterization tools to capture the microstructural information at different scales. A comprehensive SEM characterization of the high burn-up U-7Mo fuels for the research and test reactors can be found in a paper by Keiser et al in the forthcoming RRFM 2014 Transactions [4]. SEM can provide the general microstructure of the U-7Mo fuel particles, the interaction layer between the U-7Mo fuel particle and the Al-Si alloy matrix, as well as the overall bubble distribution within the fuel grains and at the fuel grain boundaries. TEM can reveal the microstructural details on both structure and composition for solid fission product distribution, fission gas bubble superlattice, defects development at the interaction layer and within the fuel particle with resolution down to ~ 1 nm.

The Reduced Enrichment Research and Test Reactor (RERTR) fuel development program is aiming to develop the reliable low-enriched fuel (U < 20%U-235) to support a safe and secured operation of the research and test reactors around the world. Fuel reactor irradiation test and the PIE are the critical part of the RERTR program. While publications or reports can be found in the open literature regarding the U-Mo fuel irradiation test and characterization, the detailed

TEM results of the irradiated fuels are still lacking [5,6,7]. Recent irradiation results from the SELENIUM test conducted in the BR-2 reactor in Belgium have shown increased fuel swelling rates for U(Mo)/Al(Si) dispersion fuel plates after a threshold fission density of ~ 4.5×10^{21} f/cm^3 [8]. In order to investigate the U-Mo fuel microstructural evolution at high fission density, it is necessary to carry out TEM characterization for the high burn-up microstructure.

Considering the threshold fission density that sets accelerated swelling rate with the break-away swelling, the microstructure detail around that turning point holds the key information about the mechanism driving the change in fuel swelling behavior and the potential mitigation that may be applied to the fuel to delay the onset of break-away swelling. It is believed that at high fission density the instability of fuel-matrix-interaction (FMI) and interlinking of large bubbles in the fuel grain are likely the causes leading to the break-away swelling. This paper focuses the recent TEM work on the high burn-up U-7Mo dispersion fuels tested in the Advance Test Reactor (ATR) at Idaho National Laboratory (INL). It is recommended to check the complement paper on the SEM high burn-up microstructure of U-7Mo for a better understanding of the TEM results.

2. Experiment

The irradiation conditions for the high burn-up U-7Mo dispersion fuels are listed in Table 1. Four sample conditions with their local fission densities at 4.5, 5.2, 5.6 and 6.3 $\times10^{21}$ fissions/cm^3 were characterized. A small 1 mm diameter fuel punch was produced from the irradiated dispersion fuel plate in a hot cell at the Hot Fuel Examination Facility (HFEF) at INL. The small punch sample was then transferred to the Electron Microscopy Laboratory. TEM samples were prepared either with conventional 3.0 mm disc sample preparation technique in a glove box or using FIB-TEM lift-out technique from an SEM sample. Schematic of 3 mm TEM disc sample preparation with a fuel punch (ϕ ~1 mm, h ~1.5 mm) and a Mo ring is shown in Figure 1. TEM characterization was performed using a 200 keV JEOL 2010 TEM/STEM system equipped with a LaB_6 filament, a Gatan UltraSacn-1000 digital camera for imaging and a Brukers Si drift detector for composition analysis with Energy Dispersive Spectroscopy (EDS). The TEM selected area diffraction (SAD) patterns from the major zones were used for structural analysis. The Java-version Electron Microscopy Simulation (JEMS) software developed by Stadelmann was used to assist in identifying the phase and indexing the diffraction patterns [9].

Table 1. Information of high burn-up dispersion fuel samples for TEM work.

Fuel plate ID	R2R010	R3R050	R0R010	R2R040
Fuel particle composition	U-7Mo	U-7Mo	U-7Mo	U-7Mo
Matrix composition	Al-2Si	Al-5Si	Pure Al	Al-2Si
U-235 enrichment (%)	19	58	58	58
Local fission density (10^{21} f/cm^3)	4.5	5.2	5.6	6.3
Fuel plate centerline temperature (°C)	105	130	122	120
TEM sample format	3 mm disc	FIB-TEM	FIB-TEM	3mm disc, FIB-TEM

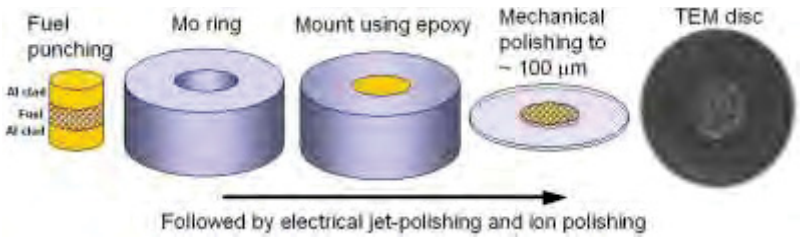

Figure 1. Schematic of TEM 3 mm disc sample preparation for irradiated dispersion fuel.

3. Results and Discussion

For fuel plate R2R010 sample with a local fission density of 4.5×10^{21} f/cm^3, the TEM work was performed on a 3 mm disc sample. Figure 2 reveals the key features of the irradiated microstructure. The overall microstructure is quite heterogeneous. From fuel particle interior to the Al alloy matrix, it typically consists of 4 different zones, namely crystalline U-Mo fuel (particle interior), a thin amorphous layer of U-Mo fuel with high Si content (3-13 at.%, fuel particle outer layer), amorphous FMI layer, and crystalline Al alloy matrix. The development of large bubbles in the U-Mo fuel particle interior and amorphous outer layer region is evident. The heterogeneous distribution of large bubbles in the FMI layer is more pronounced with area either containing just few scattered bubbles (see Figure (a)) or area filled with many bubbles (see Figure (c)). In the crystalline region of the fuel, most areas contain fission gas bubble superlattice (GBS) as shown in Figure 1 (b). It was found that the thin shell around the large bubble in the fuel is amorphous with a high content of solid fission products. No solid fission product precipitate (SFPP) was found in the areas with GBS.

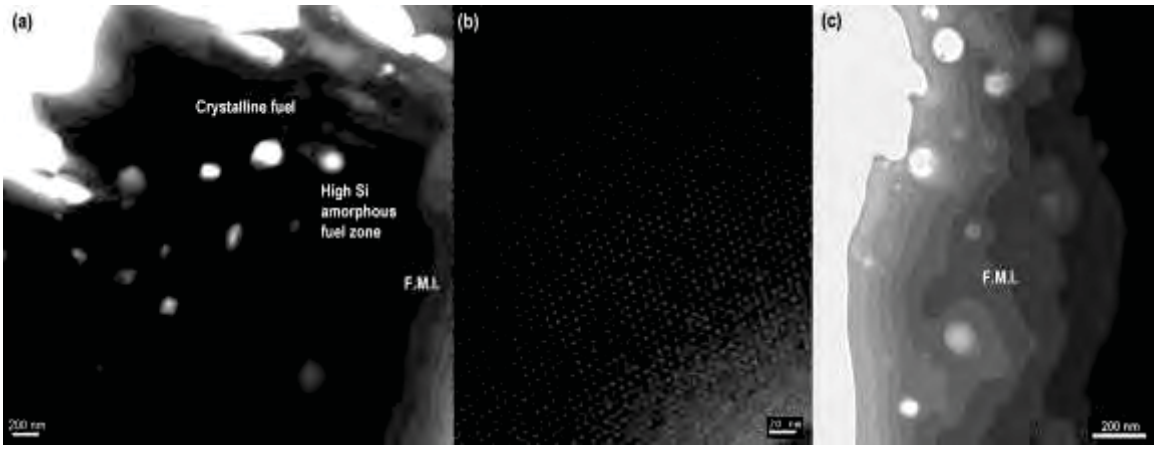

Figure 2. TEM bright field images of U-7Mo dispersion fuel (4.5×10^{21} fission/cm^3) show (a) general microstructural feature, (b) gas bubble superlattice in crystalline fuel grain and (c) another region of Fuel-Matrix-Interaction layer containing many large bubbles.

The detailed TEM analysis on GBS can be found in the previous work [2]. It is a 3D self-organized bubble superlattice with a face-center-cubic (FCC) structure coherent to the U-Mo body-center-cubic (BCC) structure. The measured average bubble size in the GBS is in the range of 3.1-3.6 nm with a superlattice constant in the range of 11-12 nm. It is believed that the crystalline U-Mo with GBS produces a high stress field in U-Mo that may significantly increase the diffusion barrier for solid fission products, therefore most solid fission products are believed to be kept in solution when the GBS is present and maintained. With the increase of solid fission product concentration in the U-Mo fuel, it could increase the solution energy, which may be one of the driving forces leading to the grain subdivision where the original large U-Mo grain (5-10 μm) breaks into much smaller submicron grains [10, 11, 12, 13]. It is intriguing that while Si addition in the Al alloy matrix seems to be effective in suppressing the growth of FMI, the diffusion of Si into the U-Mo fuel particle outer region creates an amorphous thin shell that is believed to be detrimental. The heterogeneous bubble development in the FMI layer may be related to the fluctuation of the actual local fission density as a result of imperfection of fuel particle distribution in the Al alloy matrix.

For the irradiated fuel plate R3R050 with a local fission density of 5.2×10^{21} f/cm^3, the TEM characterization was carried out on the FIB-TEM samples. The SEM data generated from the FIB-sectioned-surface provide more detailed information, compared to the conventional mechanically polished surface, which suffers from a smearing effect. Figure 3 reveals the general microstructure of the fuel particle interior with approximately 15% of the clean areas estimated from SEM. These clean areas retain crystalline structure and GBS fine bubbles as shown in the high magnification image in the middle. The measured Mo content in clean area is higher than that of the area with large bubbles (15 wt% vs. 13 wt%), indicating a more stable initial U-Mo structure. It is speculated that these clean areas may be associated with large initial grain size. The microstructural development at the fuel-matrix interface is shown in the image on the right where a white dashed line was added to mark the boundary between the amorphous and crystalline U-Mo. Compared to a sample irradiated to a fission density of 4.5×10^{21} f/cm^3, the width of the Si-rich amorphous zone increased and the bubbles with the largest size were found in this zone. It appears that the Si-rich zone grows inwards with the development of relatively large round-shaped bubbles due to surface energy constrain for the amorphous material. Another important feature is the preferential attachment of SFPP to the large bubbles as shown in Figure 4. In many cases, the SFPP formed inside the large bubbles and attached to the inner wall of the large bubbles. The EDS measurement in the STEM mode indicates these SFPP consist of Zr, Sr, Y, Ce, Ba, Nd, Pd, Te and Xe, which is different from the 5-metal: Pd, Rh, Ru, Tc and Mo found in the grain boundary bubbles in irradiated UO_2 [14]. This is likely due to the difference in diffusion kinetics of the SFP in U-Mo and UO_2 fuels.

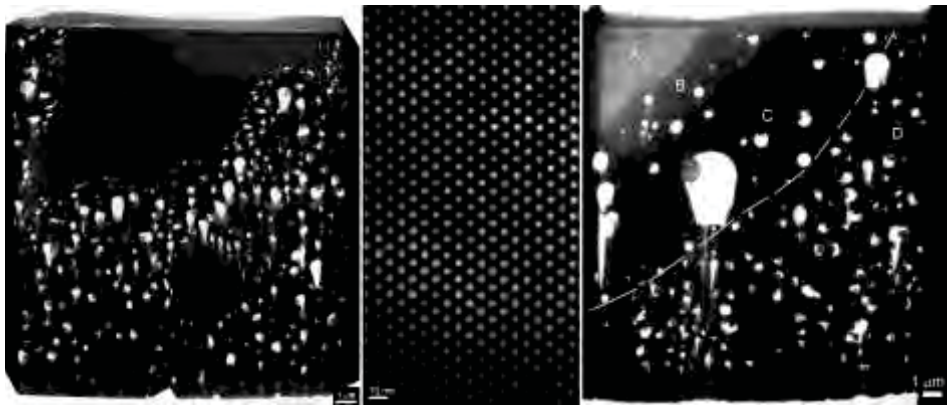

Figure 3. Bright field TEM images of irradiated U-7Mo fuel (5.2×10^{21} f/cm^3) reveal general microstructure (left), the GBS from the clean areas in the left (center), and multi-zone (right) microstructure of (A) Al alloy matrix, (B) FMI, (C) high Si amorphous zone in U-Mo and (D) crystalline fuel particle interior.

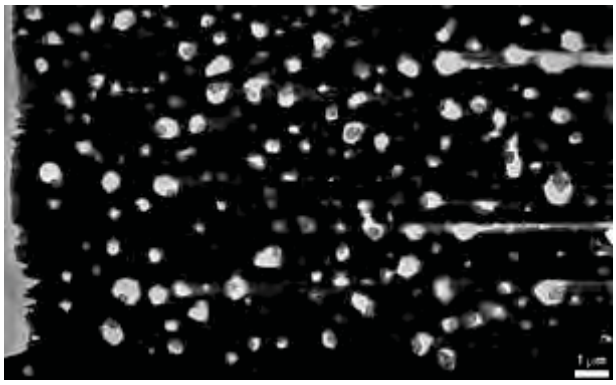

Figure 4. Low magnification TEM image of irradiated U-7Mo fuel (5.2×10^{21} f/cm^3) shows distribution of large bubbles and solid fission product precipitates preferentially attached to the large bubbles.

At this fission density, significant microstructural changes lead to the widely spread collapse of the GBS and the development of large bubbles throughout the fuel particle. The overall microstructure is still highly heterogeneous. Figure 5 reveals the development of large bubbles in the microstructural areas after GBS collapse. The EDS measurement for these areas provides the composition in wt% for U (81-86), Mo (13-16), Al (0.4-1.5) and Si (0.1-1.8). These areas are believed to remain crystalline with a GBS at the lower fission density. This is based on the composition data and the presence of a high concentration fine bubbles and the similar small bubble size in comparison to that of GBS bubbles. The formation of large bubbles after collapse of the GBS appears mainly through bubble coarsening. This is likely the mechanism that introduces large bubbles in the fuel grain interior at intermediate to high burn-up. Note that accelerated fuel plate swelling is observed in irradiated dispersion fuel plates once the average fission density reaches approximately 5×10^{21} fission/cm^3.

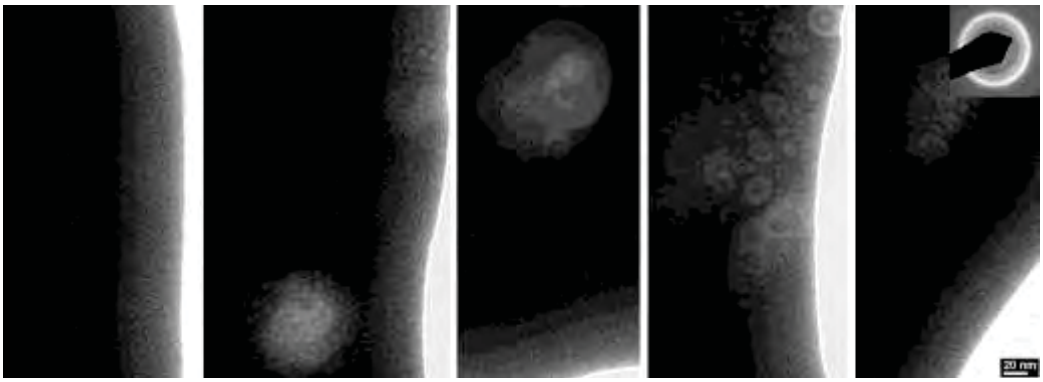

Figure 5. TEM images of neighboring amorphous areas in U-Mo fuel, revealing the development of large bubbles through bubble coarsening. Inset shows the SAD pattern from the region.

The sample made from irradiated fuel plate (R0R010) has a local fission density of 5.6×10^{21} f/cm^3. Figure 6 shows the STEM low magnification image of general microstructure on the left, and the high magnification TEM image of scattered residual GBS pocket on the right. At this fission density, although the general microstructure in the fuel particle interior looks quite similar to that of 5.2×10^{21} f/cm^3, the residual GBS was only found in small pocket in scattered areas of the crystalline region in the sample. Similar to the previous fuel plate (R3R050), the fuel interior is filled with large bubbles that exhibit a wide size range (0.1 – 1 μm). There is no evidence in TEM images of interlinking between the large bubbles. Since large bubbles tend to develop an amorphous shell filled with SFP, the increase in size and concentration of the large bubbles results in a noticeable decrease in the volume fraction of the crystalline regions of the U-Mo fuel. Note that the matrix is pure Al without Si, the Si rich amorphous outer layer did not form.

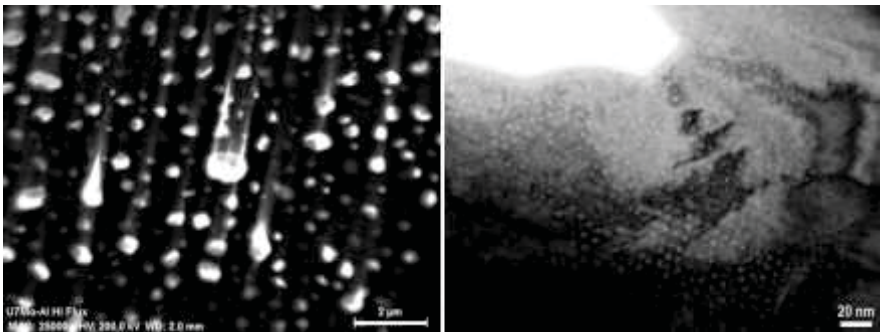

Figure 6. STEM image of the fuel particle interior for U-7Mo fuel at a fission density of 5.6×10^{21} f/cm^3 (left), and a TEM high magnification image of the residual GBS in the crystalline region (right).

The sample for fuel plate (R2R040) has the highest local fission density of 6.3×10^{21} f/cm^3. Both a conventional 3 mm disc sample and FIB-TEM samples were prepared for TEM characterization. Figure 7 shows the bright field images of an overview on the left and the detailed view of fuel interior at high magnification on the right. The SEM work identified potential interlinking of large bubbles in the fuel particle interior. The labels in the overview image on the left are for EDS composition measurement and the results are listed in Table 2. The Si-rich amorphous zone next to the FMI layer is not well defined in this case, likely the result of microstructural heterogeneities. Two important features are noticed in the high-resolution image. One is the residual GBS pocket still present in a certain part of the crystalline fuel region where the residual GBS shown in the picture was imaged at zone [100] direction. The other is the presence of fine grains known as grain subdivision, which is well known as a key microstructural feature of the rim structure in the high burn-up UO_2 pellet.

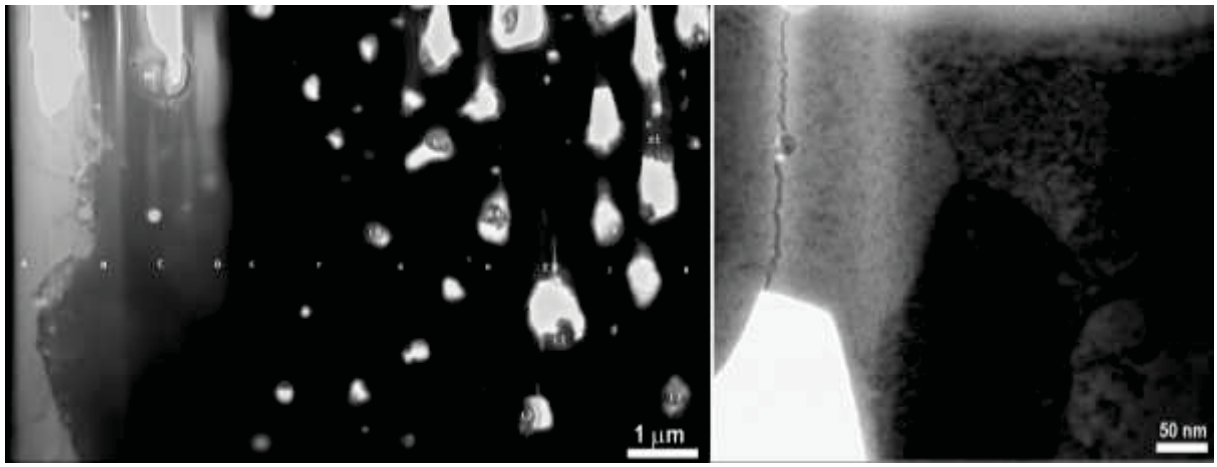

Figure 7. TEM images of irradiated U-7Mo fuel high burn-up (6.3×10^{21} f/cm^3) microstructure: overview (left) with marks for EDS composition measurement and the detailed view (right) showing grain subdivision and residual GBS.

Table 2. EDS measurement (wt%) of the spot marked in Figure 7.

ID	U	Mo	Al	Si	Other element
A	0.4	1.2	98.3	0.1	
B	52.4	6.0	34.8	6.8	
C	55.7	6.5	36.2	1.7	
D	60.2	7.5	31.8	0.5	
E	87.3	8.9	3.0	0.9	
F	88.4	9.2	0.8	1.6	
G	92.2	7.6	0	0.2	
H	91.0	8.7	0.1	0.1	
I	90.0	9.1	0.5	0.3	
J	91.7	8.1	0.1	0.2	
K	91.9	8.0	0.2	0	
L1	11.4	1.5	0.3	0	Sr_23, Ba_22, Y_19, Zr_7.6, Pd_5.6, Te_4.4, Pm_2.1
L2	5.5	0.8	0.2	0	Sr_30, Ba_37, Y_14, Zr_5.3, Pd_1.0, Te_3.0, Pm_2.1
L3	7.3	0.8	1.3	0	Sr_31, Ba_37, Y_12, Zr_6.4, Pd_0.8, Te_2.9
L4	26.2	4.7	0.3	0	Sr_23, Ba_22, Y_12, Zr_5.5, Pd_5.8, Te_1.0
L5	11.3	1.3	0.3	0	Sr_25, Ba_30, Y_15, Zr_8.7, Pd_8.0, Te_1.4
L8	16.4	4.5	0	0	Sr_29, Ba_18, Y_18, Zr_7.6, Pd_4.4
L9	10.3	0.3	0	0	Sr_32, Ba_45, Y_8.5, Zr_2.9, Pd_0.5
M1	44.2	3.4	22.6	0	Sr_2.3, Ba_0.4, Zr_27
Z1	90.0	7.9	0.2	0	Zr_1.5

For the irradiated U-7Mo fuel at high fission density, the original large fuel grains (~ 10 μm) break into much smaller grains (~ 200 nm). Unlike the original U-7Mo grain boundaries that are the preferential sites for the early development of large bubbles, the newly created boundaries from grain subdivision appear free of large bubbles other than the fine bubbles. One explanation is that these subdivided grain boundaries are mostly the small angle boundaries with low energy that is not an effective sink to attract defects, including Xe gas. This observation is consistent with that of UO_2 high burn-up rim structure [15]. EDS data in Table 2 indicates that most SFPPs associated with large bubbles consist of Sr, Ba, Y, Zr and Pd. The general microstructure of the fuel particle interior is a mixture of amorphous and crystalline regions as shown in Figure 8. Bubble coarsening continues in the amorphous region (image on the left), and small pockets of GBS can still be observed (image on the right).

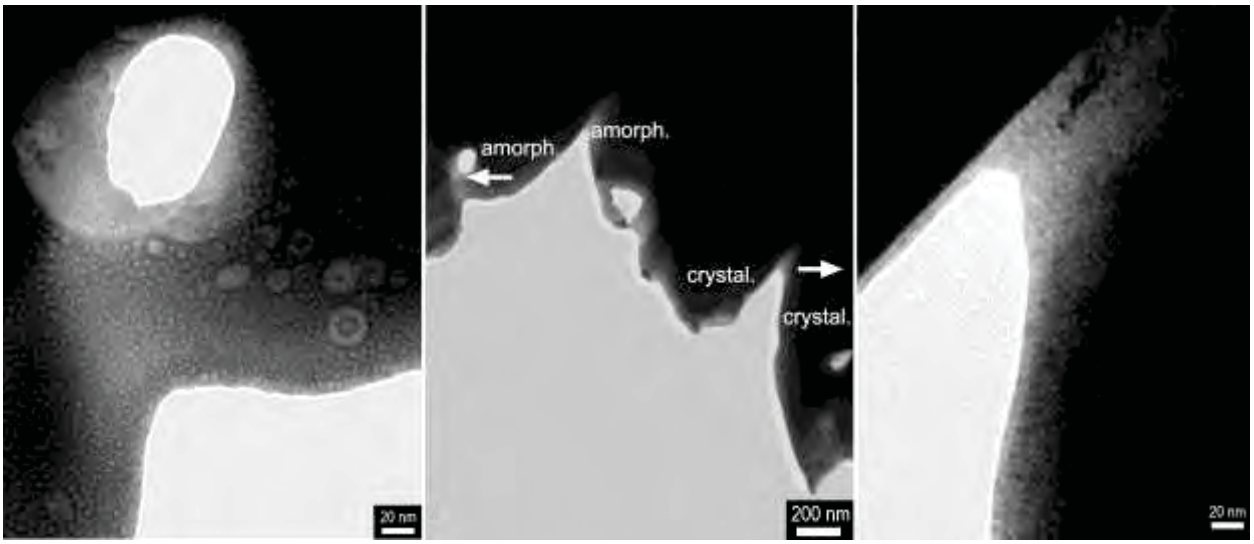

Figure 8. TEM image of high burn-up (6.3×10^{21} f/cm^3) U-7Mo fuel microstructure (middle) showing the mixture of amorphous region with bubbles (left) and the crystalline region with residual GBS (right). The light contrast around the large bubbles consists of high concentration solid fission products.

From the SEM work, it was found that at high burn-up, the development of large bubbles appears more pronounced around the grain boundaries. This appears to combine with the bubble coarsening occurring in the fuel, which seems to be the driving mechanism for the large bubble development. Linkage of large bubbles becomes evident at high burn-up. The interlinkage of large bubbles is attributed to the increase of large bubble concentration and the growth of large bubbles. It is speculated that when the microstructure is filled with a high concentration of large bubbles or linked bubbles, the vacancy partitioning to bubble growth becomes important, and the fuel swelling is then dominated by the vacancy production from irradiation rather than from fission gas and SFP production. One supporting evidence is that the break-away swelling occurs when fuel reaches high burn-up with reduced fission rate.

As most of the research and test reactors are the thermal neutron spectrum reactors, the additional fissions from Pu-239 as a result of U-238 transmutation has to be considered in fuel microstructure development. This effect may be associated with the fuel format, geometry and irradiation configuration in the reactor core. It is often called fission “peaking effect” which could lead to a local fission density much higher than eastimeted from U-235 from the Plate Code [16]. Besides the “peaking effect” from fuel plate geometry, which is anticipated to be similar for both dispersion fuel and monolithic fuel, the dispersion fuel is expected to have a stronger “peaking

effect" due to its larger surface to volume ratio for fuel particles in comparison to monolithic fuel foil for the comparable U-Mo fuel volume. This could be the partial explanation for the early break-away swelling observed in dispersion fuel, compared to what has been observed for monolithic fuel. Another major difference between dispersion and monolithic fuel is the fact that the U-7Mo particles in dispersion fuel compared to the U-10Mo foil in monolithic fuel are a thermodynamically less stable phase. The heterogeneous distribution of the dispersed U-7Mo fuel particles in as-fabricated dispersion fuel may also be partially responsible for the non-uniform irradiated microstructure from particle to particle, although the estimated local fission density is the same. This is because the Plate Code assumes a uniform particle distribution for a fission density calculation.

4. Conclusions

The high burn-up microstructure of irradiated U-7Mo dispersion fuels is dominated by large bubbles with size ranging from a few hundred nm to ~ 1 μm. Bubble coarsening is identified as an important mechnism in the devlopment of large bubbles. At a fission density of 5.2×10^{21} f/cm^3, there is roughly 15% of the particle area (clean fuel grain) that contains only the gas bubble superlattice of ~ 3.5 nm bubbles without large bubbles. The size of these areas varies from few μm up to more than ~ 10 μm. Small pockets of GBS bubbles are still present in the crystalline region at the highest fission density of 6.3×10^{21} f/cm^3, but with significantly reduced volume fraction, and the GBS pocket size is typically around a few hundred nm or below. The early development of large round bubbles is evident in the high Si amorphous layer next to the fuel-matrix-interaction layer. At high fission density, a significant portion of the original U-7Mo grains turn amorphous as a result of radiation-induced atomic displacement damage from high energy fission fragments as well as the local composition change due to fission product generation. The collapes of the GBS at high burn-up results in a rapid precipitation of the solid fission products at a thin amorphous shell around the large bubbles or inside the large bubbles. The observed microstructures from TEM analysis of high burn-up U-7Mo dispersion fuel plate samples has helped identify possible mechanisms for the eventual break-away swelling of U-7Mo fuel at high fission density.

Acknowledgments

This work was supported by the U.S. Department of Energy, Office of Nuclear Materials Threat Reduction (NA-212), National Nuclear Security Administration to the RERTR program, under DOE-NE Idaho Operations Office Contract DE-AC07-05ID14517. Accordingly, the U.S. Government retains a nonexclusive, royalty-free license to publish or reproduce the published form of this contribution, or allow others to do so, for U.S. Government purposes.

References

[1] S. Van den Berghe, W.Van Renterghhem, A. Leenaers, J. Nucl. Mater., 375 (2008) 340-346.
[2] J. Gan, D.D. Keiser Jr., D.M. Wachs, A.B. Robinson, B.D. Miller, T.R. Allen, J. Nucl. Mater., 396 (2010) 234-239.
[3] B.D. Miller, J. Gan, J. Madden, J.F. Jue, A. Robinson, D.D. Keiser, Jr., J. Nucl. Mater., 424 (2012) 38-42.
[4] D.D. Keiser, Jr., J.F. Jue, J. Gan, B.D. Miller, A.B. Robinson, P. Medvedev and D.M. Wachs, "High Burn-up Microstructure of U-7Mo Alloy", to be published in RRFM 2014 Transaction,

[5] A. Leenaers, S. Van den Berghe, J. Van Eyken, E. Koonen, F. Charollais, P. Lemoine, Y. Calzavara, H. Guyon, C. Jarousse, D. Geslin, D. Wachs, D. Keiser, A. Robinson, G. Hofman, Y.S. Kim, J. Nucl. Mater., 441 (2013) 439-448.
[6] S. Van den Berghe, Y. Parthoens, F. Charollais, Y.S. Kim, A. Leenaers, E. Koonen, V. Kuzminov, P. Lemoine, C. Jarousse, H. Guyon, D. Wachs, D. Keiser Jr, A. Robinson, J. Stevens, G. Hofman, J. Nucl. Mater., 430 (2012) 246-258.
[7] A. Leenaers, S. Van den Berghe, W. Van Renterghem, F. Charollais, P. Lemoine, C. Jarousse, A. Röhrmoser, W. Petry, J. Nucl. Mater., 412 (2011) 41-52.
[8] S. Van den Berghe, Y. Parthoens, G. Cornelis, A. Leenaers, E. Koonen, V. Kuzminov, C. Detavernier, J. Nucl. Mater., 442 (2013) 60-68.
[9] P. Stadelmann, http://cimewww.epfl.ch/people/stadelmann/jemsWebSite/jems.html.
[10] L. E. Thomas, C. E. Beyer, L. A. Charlot, J. Nucl. Mater., 188 (1992) 80-89.
[11] S. E. Donnelly, J. H. Evans, [ed.]. NATO Advanced Research Workshop on Fundamental Aspects of Inert Gases in Solids. New York : Plenum Press, 1191.
[12] L. M. Clarebrough, M. E. Hargreaves, M. H. Loretto. *Recovery and Recrystallization of Metals.* New York : Interscience, 1963.
[13] J-P. Crocombette, J. Nucl. Mater., 305 (2002) 29-36.
[14] Hj. Matzke and H. Blank, J. Nucl. Mater. 166 (1989) 120.
[15] I.L.F. Ray, Hj. Matzke, H.A. Thiele, M. Kinoshita, J. Nucl. Mater., 245 (1997) 115-123.
[16] Y. S. Kim, G.L. Hofman, P. G. Medvedev, G. V. Shevlyakov, A. B. Robinson, H. J. Ryu, 2006 International Meeting on Reduced Enrichment for Research and Test Reactors, “Post Irradiation Analysis and Performance Modeling of Dispersion and Monolithic U-Mo Fuels”.